An ab Initio MO Study on Fragmentation Reaction Mechanism of Thymine Dimer Radical Cation

Misako Aida,*,† Fukiko Inoue,† Motohisa Kaneko,† and Michel Dupuis‡,§

Contribution from the Biophysics Division, National Cancer Center Research Institute, 5-1-1 Tsukiji, Chuo-ku, Tokyo 104, Japan, and IBM Corporation, 375 South Road, Poughkeepsie, New York 12601

Received January 21, 1997. Revised Manuscript Received September 23, 1997[⊗]

Abstract: Ab initio CASSCF calculations with the 6-31G basis set are reported for the fragmentation reaction of thymine dimer radical cation. The unpaired electron of thymine dimer radical cation is localized on the lengthened C6−C6′ bond, and the fragmentation starts with the cleavage of this bond. The puckering of the cyclobutane ring (C6−C6′−C5′−C5) leads to one of the C6 atoms being pyramidal and the other being planar in the initial thymine dimer radical cation structure. During the C6−C6′ bond breaking step, the pyramidal C6 takes on a sp^3 hybridization to accept the localized unpaired electron; the planar C6′ takes on a sp^2 hybridization with an empty p orbital. In the next step of the fragmentation, the breaking of the C5−C5′ bond, the localized unpaired electron on C6 pairs up with one of the electrons formerly of the C5−C5′ bond to form a neutral thymine monomer while the other electron of the C5−C5′ bond moves to the other ring to form a thymine radical cation. The reaction proceeds stepwise and exothermally. The puckering of the cyclobutane ring of thymine dimer plays an important role in determining the fragmentation path and the spin distribution at the final stacked pair.

Introduction

The formation of the cyclobutadipyrimidines (pyrimidine dimers, Pyr<>Pyr) by far-UV (200−300 nm) irradiation in DNA is toxic and mutagenic to the living cells. One of the repair processes to remove the DNA photoproducts is the photoreactivation by exposure to near-UV and visible light (300−500 nm): pyrimidine dimers are reactivated into individual bases by DNA photolyases, which utilize near-UV and visible light to initiate the photocycloreversion reaction. Photolyases have been shown to exist in many species.[1,2] The three-dimensional crystallographic structure of DNA photolyase from *Escherichia coli* appeared recently.[3] It is thought that the dimer splitting proceeds thermally following a photoinduced electron transfer to or from the dimer. From thermodynamical estimates and isotopic effects in the fragmentation process, it is generally accepted[4−9] that the dimer splitting may be a consequence of a single electron transfer to the dimer from the electronically excited chromophore (FAD) sensitized by the photoexcited antenna chromophore in the enzyme. The enzymatic reaction most likely proceeds via the radical anion pathway. High-level MO calculations on the fragmentation of the cation and the anion should provide significant insights as to why the enzyme system favors one pathway over the other.

Photoinduced oxidation also plays an importnat role in initiating the pyrimidine dimer splitting. Recently, it was found that the intercalating complexes of rhodium(III), which are photooxidants and which bind tightly to DNA, catalyzed the repair of a thymine dimer.[10] The repair was initiated by photoinduced oxidation and thus is found to proceed through a radical cation. Repair of dimer-containing DNA duplex can be accomplished with sunlight and a catalytic amount of metal complex, which are intercalated at a remote position. This process might be relevant to potential DNA repair therapies. Thus a detailed theoretical understanding of the structures and energetics of the dimer cation fragmentation should provide as well here invaluable insight into this very significant experimental finding.

Experimental model studies have demonstrated that both the photodimer radical anion and cation undergo facile fragmentation reactions.[11−14] The exact mechanism of the fragmentation, however, is not yet clearly understood for each of the dimer radicals, from the aspect of why the fragmentation reaction, in which orbital symmetries are not retained in going from reactant to product, proceeds thermally.

The cycloaddition of two ethylenes or the cycloreversion of cyclobutane is one of the textbook examples used in the illustration of the Woodward−Hoffman rules[15] of orbital symmetry. The studies on the cyclobutane radical cation[16,17]

* To whom correspondence should be addressed.
† National Cancer Center Research Institute.
‡ IBM Corporation.
§ Present address: Pacific Northwest National Laboratory, EMLS/K1-90, Battelle Blvd, Richland, WA 99352.
⊗ Abstract published in *Advance ACS Abstracts,* December 1, 1997.

(1) Sancar, G. B. *Mutat. Res.* **1990**, *236*, 147−160.
(2) Sutherland, B. M.; Bennett, P. V. *Proc. Natl. Acad. Sci. U.S.A.* **1995**, *92*, 9732−9736.
(3) Park, H.-W.; Kim, S.-T.; Sancar, A.; Deisenhofer, J. *Science* **1995**, *268*, 1866−1872.
(4) Sancar, A. *Biochemistry* **1994**, *33*, 2−9.
(5) Okamura, T.; Sancar, A.; Heelis, P. F.; Begley, T. P.; Hirata, Y.; Mataga, N. *J. Am. Chem. Soc.* **1991**, *113*, 3143−3145.
(6) Kim, S.-T.; Sancar, A.; Essenmacher, C; Babcock, G. T. *J. Am. Chem. Soc.* **1992**, *114*, 4442−4443.
(7) Pouwels, P. J. W.; Kaptein, R. *Appl. Magn. Reson.* **1994**, *7*, 107−113.
(8) Heelis, P. F.; Hartman, R. F.; Rose, S. D. *Chem. Soc. Rev.* **1995**, *24*, 289−297.
(9) Scannell, M. P.; Fenick, D. J.; Yeh, S.-R.; Falvey, D. E. *J. Am. Chem. Soc.* **1997**, *119*, 1971−1977.
(10) Dandliker, P. J.; Holmlin, R. E.; Barton, J. K. *Science* **1997**, *275*, 1465−1468.
(11) Lamola, A. A. *Mol. Photochem.* **1972**, *4*, 107−133.
(12) Burdi, D.; Begley, T. P. *J. Am. Chem. Soc.* **1991**, *113*, 7768−7770.
(13) Diogo, H. P.; Dias, A. R.; Dhalla, A.; Minas da Piedade, M. E.; Begley T. P. *J. Org. Chem.* **1991**, *56*, 7340−7341.
(14) McMordie, R. A. S.; Begley, T. P. *J. Am. Chem. Soc.* **1992**, *114*, 1886−1887.
(15) Woodward, R. B.; Hoffmann, R. *Angew. Chem., Int. Ed. Engl.* **1969**, *8*, 781−853.
(16) Pabon, R. A.; Bauld, N. L. *J. Am. Chem. Soc.* **1984**, *106*, 1145−1146.

S0002-7863(97)00184-4 CCC: $14.00

showed a low activation energy for the cycloaddition of ethylene and the ethylene radical cation, in remarkable contrast with the high activation energy for the corresponding neutral reaction.[18] The dissociation reaction of cyclobutane radical cation is endothermic. No ab initio MO study exists for the energetics in the dissociation of pyrimidine dimer radical cation. Although there is a cyclobutane ring in the pyrimidine dimer, its electronic structure is likely to be different from cyclobutane itself, because of the presence of the two pyrimidine rings.

With the goal of characterizing the repair process of a thymine dimer, it is necessary to obtain a description of the reaction profiles of the fragmentation of both the pyrimidine dimer radical cation and radical anion. In this article, we describe the reaction profile of the fragmentation of the thymine dimer radical cation using ab initio MO theory. It is shown that the fragmentation reaction of thymine dimer radical cation is exothermic, and proceeds stepwise. Because of the unusual diffuse dipole-bound character of the thymine dimer radical anion, special care must be taken for the calculations including the inclusion of Rydberg functions. The details will be reported soon.

Methods

The complete active space (CAS) SCF calculations with geometry optimization were carried out to obtain the fragmentation pathway of thymine dimer radical cation. The fragmentation of thymine dimer radical cation is the cycloreversion of the cyclobutane ring, which corresponds to the conversion of the two σ bonds (the C5−C5′ σ bond and the C6−C6′ σ bond of thymine dimer radical cation) to the two π bonds (the two C5═C6 π bonds of the two thymine monomers). A bonding orbital and an antibonding orbital are associated with each of the bonds and, in the case of the dimer cation, three electrons are actively involved in the bond breaking/bond formation process as the reaction proceeds from dimer to fragment. A CAS wave function made up of all the Slater determinants obtained by distributing the three active electrons among the four active orbitals in all possible ways consistent with spin and spatial symmetry (CAS(3e+4o)), is expected to provide a semiquantitative description of the cycloreversion of the thymine dimer radical cation. The calculations were performed with the 6-31G basis set,[19] using the HONDO program.[20]

Initially an approximate reaction pathway was constructed. With the structure of the thymine dimer[21] and the structure of two thymine molecules in their stacked arrangement in B DNA[22] as starting points, the structures for the cationic species were obtained. A linearized synchronous transit pathway (LST) was constructed between these initial and final structures by allowing all the geometrical parameters to vary simultaneously as a fraction of their total change between the dimer cation and the fragment cation. The reaction pathway obtained in this manner was subsequently refined to yield key geometrical structures of the fragmentation mechanism. Two local minima and two transition state structures were identified, by means of a full analysis of the vibrational modes at these stationary points.

Results

Structure of Thymine Dimer Radical Cation. First in this work, we have optimized the geometry, at CAS(3e+4o) level, of thymine dimer radical cation (T<>T(•+)) which is obtained by the removal of an electron from the neutral thymine dimer (T<>T). The optimized geometry is shown in Figure 1 with the atomic labels. As in the neutral T<>T, the four-membered ring in T<>T(•+) is puckered. This structure is labeled TTp-1. The torsional angles around the four-membered ring are listed in Table 1.

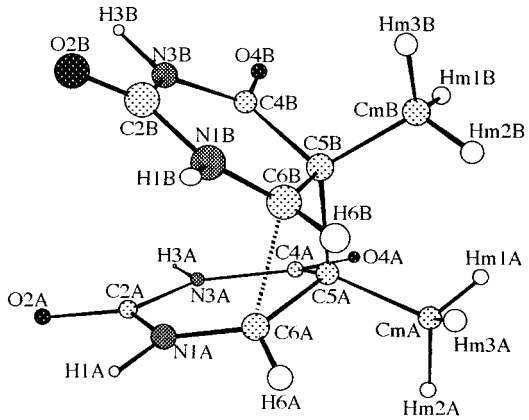

Figure 1. Structure of thymine dimer radical cation with atomic labels.

Table 1. Torsional Angles (in degrees) around the Four-Membered Rings in TTp-1 and ts-66[a]

	TTp-1	ts-66
C5A−C5B−C6B−C6A	−16.54	−18.39
C5B−C6B−C6A−C5A	18.07	20.36
C6B−C6A−C5A−C5B	−16.53	−18.50
C6A−C5A−C5B−C6B	23.58	27.83
CmA−C5A−C5B−CmB	26.40	29.54
C4A−C5A−C5B−C4B	24.60	29.18
N1A−C6A−C6B−N1B	21.21	25.50
H6A−C6A−C6B−H6B	20.53	21.08
CmA−C5A−C6A−C6B	102.09 (ax)	100.33 (ax)
C4A−C5A−C6A−C6B	−134.85 (eq)	−137.07 (eq)
H6A−C6A−C5A−C5B	−106.01 (eq)	−109.83 (eq)
N1A−C6A−C5A−C5B	96.43 (ax)	93.06 (ax)
CmB−C5B−C6B−C6A	−137.90 (eq)	−139.68 (eq)
C4B−C5B−C6B−C6A	101.39 (ax)	100.60 (ax)
H6B−C6B−C5B−C5A	73.27 (ax)	66.93 (ax)
N1B−C6B−C5B−C5A	−131.24 (eq)	−129.80 (eq)

[a] Atomic labels are shown in Figure 1. The axial and equatorial relative to the four-membered ring are indicated by (ax) and (ex), respectively.

Because of the puckering of the four-membered ring, the two thymine rings in T<>T(•+) are not identical. It is convenient to distinguish the rings: ring A denotes the lower ring when the molecule is placed as in Figure 1, and ring B denotes the upper ring. The distinction is helpful for the description of the fragmentation mechanism later on.

Fragmentation Pathway. Along the fragmentation path from the initial dimer radical cation (TTp-1) to the stacked pair in DNA, the structures of the stationary points are drawn in Figure 2. The stationary points are labeled ts-66, TTp-2, and ts-55, which correspond to the transition state for the C6A−C6B bond breaking, the stretched bond isomer of TTp-1, and the transition state for the C5A−C5B bond breaking, respectively. T(•+):T in Figure 2 denotes the final "stacked" structure in B-DNA. The energies of the structures along the dissociation path are summarized in Table 2. The four-membered ring in ts-66 is also puckered. The torsional angles around the four-membered ring in ts-66 are listed in Table 1. The bond lengths and the bond indices around the four-membered ring for each of the structures along the dissociation path are summarized in Table 3. The angle of the H6 atom with the C6−N1−C2 plane for each of the rings is also summarized in Table 3 for each of the structures along the dissociation path. The spin populations on the four-membered ring are summarized in Table 4. The

(17) Jungwirth, P.; Bally T. *J. Am. Chem. Soc.* **1993**, *115*, 5783−5789.
(18) Bernardi, F.; Bottoni, A.; Robb, M. A.; Schlegel, H. B.; Tonachini, G. *J. Am. Chem. Soc.* **1985**, *107*, 2260−2264.
(19) Hehre, W. J.; Ditchfield, R.; Pople, J. A. *J. Chem. Phys.* **1972**, *56*, 2257−2261.
(20) Dupuis, M.; Marquez, A.; Davidson, E. R. *HONDO 95.3 from CHEM-Station*; IBM Corporation: Kingston, NY, 1995.
(21) Aida, M.;Kaneko, M.;Dupuis, M. *Int. J. Quantum Chem.* **1996**, *57*, 949−957.
(22) Leonard, G. A.; Booth, E. D.; Hunter, W. N.; Brown, T. *Nucleic Acids Res.* **1992**, *20*, 4753−4759.

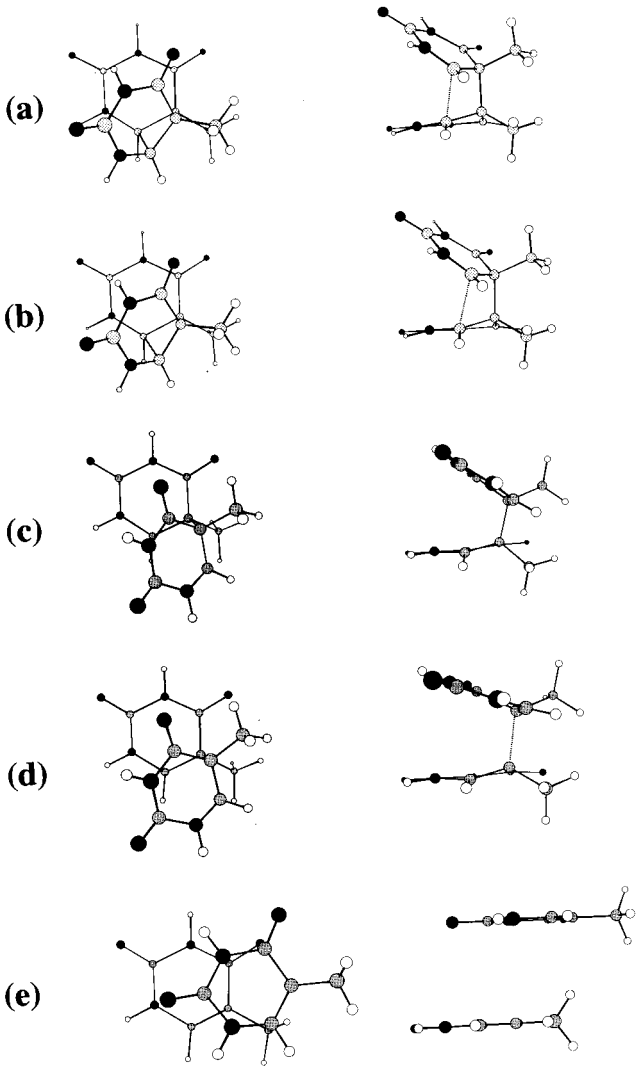

Figure 2. Structures of the stationary points along the fragmentation path of thymine dimer radical cation. Views from two directions are drawn: (a) TTp-1, (b) ts-66, (c) TTp-2, (d) ts-55, and (e) T(•+):T.

Table 2. CAS(3e+4o) Energies of T<>T(•+) along the Dissociation Path[a]

	relative energy[b]
TTp-1	0.0
ts-66	0.26
TTp-2	−4.56
ts-55	−3.14
T(•+):T	−29.41

[a] See Figure 2 for the conformations of the stationary states along the dissociation path. [b] In kcal/mol.

electron contour maps of the singly occupied highest molecular orbital (SOMO) and the doubly occupied highest molecular orbital (HOMO) for each of the points are drawn in Figure 3. The points e, f, and g in Figure 3 are the intermediate points on the linear synchronous transition paths connecting ts-55 and T(•+):T. The occupation numbers for the natural orbitals of SOMO and HOMO along the dissociation path are also given in Table 4. The fragmentation pathway thus characterized is shown schematically in Figure 4.

Discussion

Initial Thymine Dimer Radical Cation. Our previous RHF calculation on thymine dimer showed[21] that the ring fusion at the C5 and C6 atoms of two thymine bases created the four-

Table 3. Bond Lengths (in Å), Bond Indices, and Torsional Angles (in degrees) around the Four-Membered Ring[a] along the T<>T(•+) Dissociation Path[b]

	bond length				bond index				torsional angle	
	C5A−C5B	C6A−C6B	C5A−C6A	C5B−C6B	C5A−C5B	C6A−C6B	C5A−C6A	C5B−C6B	∠(H6A−C6A−N1A−C2A)	∠(H6B−C6B−N1B−C2B)
TTp-1	1.640	2.153	1.521	1.516	0.80	0.27	0.89	0.88	−151.07	169.15
ts-66	1.642	2.265	1.517	1.510	0.80	0.21	0.91	0.88	−143.86	174.67
TTp-2	1.676	3.028	1.502	1.485	0.80	0.00	0.93	0.93	−146.02	178.78
ts-55	1.902	3.162	1.457	1.448	0.60	0.00	1.03	1.02	−162.60	174.50
T(•+):T	4.122	4.399	1.348	1.419	0.00	0.00	1.67	1.16	180.00	180.00

[a] See Figure 1 for the atomic labels. [b] See Figure 2 for the conformations of the stationary points along the dissociation path.

Table 4. Spin Populations of the Four-Membered Ring[a] and Occupation Numbers for the Natural Orbitals along the T<>T(•+) Dissociation Path[b]

	spin population				occupation number[c]	
	C5A	C6A	C5B	C6B	SOMO	HOMO
TTp-1	0.06	0.37	0.07	0.33	0.998	1.973
ts-66	0.06	0.55	0.07	0.20	0.998	1.973
TTp-2	0.05	0.84	0.08	0.01	1.000	1.973
ts-55	0.11	0.70	0.16	0.05	1.001	1.952
T(•+):T	0.14	0.14	0.62	0.15	1.000	1.924

[a] See Figure 1 for the atomic labels. [b] See Figure 2 for the conformations of the stationary points along the dissociation path. [c] See Figure 3 for the electron contour maps.

membered cyclobutane ring which is puckered. The puckering leads to axial or equatorial directions for the substituent atoms on the cyclobutane ring: the substituent atoms on the two thymine bases differ in their direction. Especially noteworthy is the direction of the H6A atom. In the neutral T<>T, the H6A atom is equatorial relative to the four-membered ring and axial relative to the π conjugation system in the planar N1(H1)−C2(O2)−N3(H3)−C4(O4) moiety in ring A. Therefore, electrons on the C6A−H6A bond participate in the stabilization of the π system (*i.e.*, hyperconjugation). The highest occupied molecular orbital (HOMO) of the neutral T<>T is localized on the C6A−C6B bond.

After ionization, the SOMO orbital of TTp-1 is localized on the C6A−C6B bond (see Figure 3a), and the bond is lengthened (see Table 3) compared to the neutral species, as the bond is now weaker due to the single electron occupancy. The four-membered ring in TTp-1 is puckered (see Table 1), as in the neutral species. The relative orientations of the H6A atom in TTp-1 are similar to those in the neutral T<>T. Electrons on the C6A−H6A bond participate in the stabilization of the π system. The slightly higher spin population on the C6A atom than that on the C6B atom (see Table 4) is probably caused by this effect. The puckering of the cyclobutane ring brings about the difference in the electronic structures in the two thymine rings and it plays an important role in determining the dissociation path as will be described later.

Structural Change and Spin Distribution Change Along the Fragmentation Path. The cyclobutane ring (C5A−C5B−C6B−C6A) in the thymine dimer radical cation changes to two ethylene moieties (C5A═C6A and C5B═C6B) after the fragmentation: each of the C atoms in the cyclobutane ring changes its character from pyramidal sp^3 to planar sp^2. The dissociation starts with the breaking of the weak C6A−C6B bond which is made up of one electron only. At ts-66, the transition state in the C6A−C6B bond breaking step, the spin population on C6A becomes larger than that on C6B (see Figure 3b and Table 4); the σ-like orbital on C6A−C6B turns into the localized orbital on C6A, not on C6B. This specificity originates in the puckering of the four-membered ring of neutral thymine dimer. As stated before, in the neutral thymine dimer, because of the puckering, the H6A atom is axial and the H6B atom is equatorial relative to ring A and ring B, respectively.[21] After the ionization, TTp-1 keeps these characteristics (see Tables 1 and 3, and Figure 2a). The puckering forces the C6A atom to be pyramidal (sp^3-like) and the C6B atom to be planar (sp^2-like). Along the C6A−C6B bond breaking, the unpaired electron moves to the C6A atom to form the tetrahedral sp^3 hybrid; the C6B atom turns planar with the electron deficient sp^2 hybrid which is stabilized by the π-conjugated system in ring B (see Figure 3c and Table 4). The initial structural characteristics controls the direction of the electron movement along the dissociation path, and on which C6 atom the electron is localized at TTp-2.

During the next C5A−C5B bond dissociation step, one of the two electrons of the C5A−C5B bond at TTp-2 pairs up with the localized electron on C6A to form the π orbital on C5A−C6A; the other electron of the C5A−C5B bond moves to the B ring and forms the half-occupied π orbital on C5B−C6B in T(•+) (see Figure 3c−h). As a whole, the A ring, which has a slightly high spin density on C6A at the initial thymine dimer radical cation (TTp-1), turns to a neutral thymine, and the B ring turns to a thymine radical cation after the dissociation.

The inversion of the cyclobutane ring leads to another isomer, which is a mirror image of the one described in Figure 1. They are intrinsically the same as long as only the thymine dimer is taken into account. In DNA or in an oligonucleotide, however, the rings in thymine dimer must be distinguished because of the main chain direction. The structure in Figure 1 is drawn so that the main chain (5′ → 3′) runs from the top to the bottom of the figure when the thymine dimer is a part of DNA.

Throughout the fragmentation reaction, the occupation numbers of SOMO and HOMO are almost equal to one and two, respectively (see Table 4). It indicates that the reaction is essentially well described by a single determinant.

The fragmentation pathway of thymine dimer radical cation is shown schematically in Figure 4. As described above, our CAS calculations indicate that the puckering of the cyclobutane ring of the thymine dimer plays a critical role in determining the spin and charge distribution along the fragmentation path. These characteristics were not revealed in the recent work by Voityuk *et al.*[23] using the semiempirical AM1 UHF method. They described that the AM1 method yielded a pyrimidine dimer structure with a planar four-membered ring and that removing an electron from the dimer immediately induced the cleavage of the C6−C6′ bond. Their fragmentation mechanism is different from the one presented here. They were unable to locate any stationary points for the dimer radical cation containing a cyclobutane-like ring; they found a structure with the two thymine bases held together by the C5−C5′ bond. In contrast, we find the two local minima (TTp-1 and TTp-2 in Figures 2 and 4) for the dimer radical cation, although the barrier between TTp-1 and TTp-2 is rather low (Table 2).

Comparison with the Case of $(C_2H_4)_2^{\bullet+}$ Complex. The $C_4H_8(\bullet+)$ potential energy surface was studied by Jungwirth *et al.*[17,24] at the level of QCISD(T)/6-31G*//UMP2/6-31G*. They showed that the ring opening reaction of cyclobutane radical cation was endothermic by more than 20 kcal/mol. A π complex cation intermediate was shown to exist, where the two ethylene molecules were linked by a single bond of ∼1.9 Å and which was bound by 18.2 kcal/mol relative to ethylene + ethylene(•+). They also showed that the large discrepancies existed between the UHF- and UMP2-optimized geometries of the cyclobutane radical cation. At the UHF level, a trapezium was found to be the most stable structure; at the UMP2 level, it turned out that a rhombus structure was the most stable. At both of the levels, it was shown that the long-bond trapezoidal structure was favored by the influence of electron-releasing substituents. Since the long bond is made up with only one electron, it is probable that the electron-releasing substituent stabilizes the trapezoidal structure.

In the present case of T<>T(•+), the cyclobutane ring in TTp-1 shows a long-bond trapezoidal structure at the CASSCF level of theory. The substituents to the C6 atoms are the N1

(23) Voityuk, A. A.; Michel-Beyerle, M.-E.; Rösch, N. *J. Am. Chem. Soc.* **1996**, *118*, 9750−9758.
(24) Jungwirth, P.; Carsky, P.; Bally T. *J. Am. Chem. Soc.* **1993**, *115*, 5776−5782.

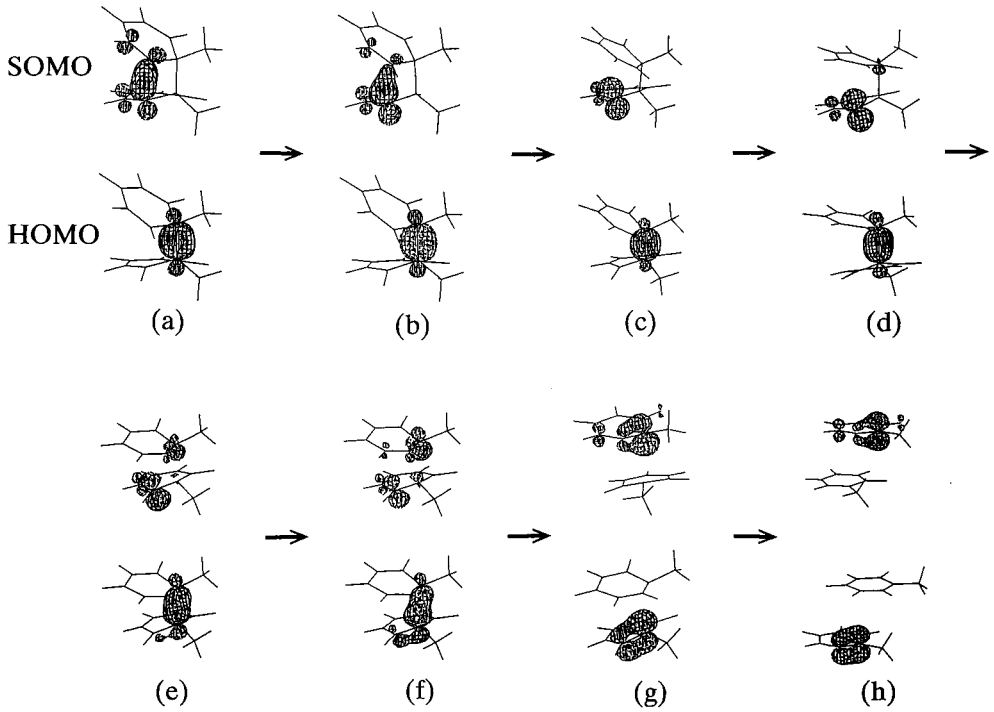

Figure 3. Electron contour maps of SOMO and HOMO along the fragmentation path of thymine dimer radical cation: (a) TTp-1, (b) ts-66, (c) TTp-2, (d) ts-55, (h) T(•+):T, and (e−g) the intermediates of the linear synchronous transition paths connecting ts-55 and T(•+):T.

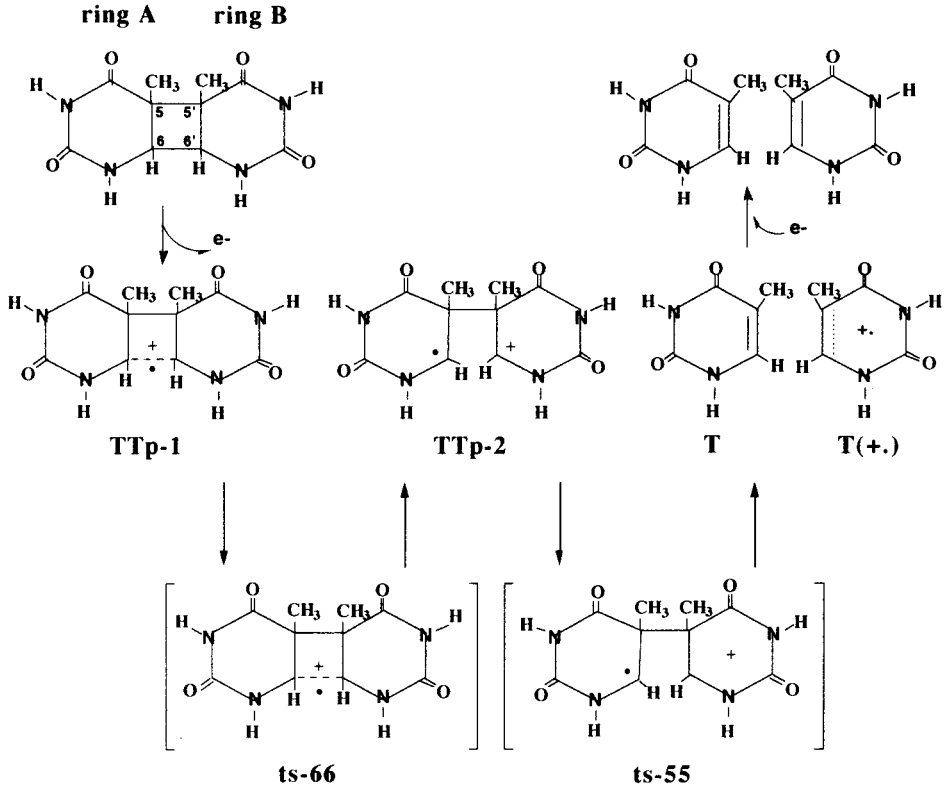

Figure 4. Schematic description of the fragmentation path of thymine dimer radical cation.

atoms, and those to the C5 atoms are the methyl groups and the C4 atoms of the carbonyl groups. The nitrogen atom and the methyl group are electron releasing, while the carbonyl group is electron withdrawing. Thus the electron-releasing effect to the C6 atoms is larger than that to the C5 atoms: it follows that the trapezoidal structure with the long C6−C6′ bond is thus favored. The structure obtained at the CAS(3e+4o) level of theory would not change qualitatively with a higher level calculation, on account of the substituents of the cyclobutane ring in thymine dimer.

The cycloreversion reaction of the cyclobutane radical cation is highly endothermic at any level of the calculations.[17] A transition state was specified between the cyclobutane radical cation (cB •+) and the π complex cation intermediate, although no transition state was described between the π complex cation intermediate and the infinite system (ethylene + ethylene(•+)).[17] In contrast, the cycloreversion reaction of the thymine dimer radical cation is exothermic at the CASSCF level of theory as shown in Table 2. Compared to the cB •+ case, the π conjugation in thymine is responsible for the greater stabilization

of the monomer cation, thus making the reaction exothermic. To estimate the dynamic electron correlation effect, we carried out MP2 calculations preliminarily for TTp-1 and T(•+):T. The exothermicity was reduced to 5.0 kcal/mol. Since the number of the bonds in TTp-1 is larger than that in T(•+):T, TTp-1 is much more stabilized by the dynamical electron correlation effects than T(•+):T is.

Comparison with Experiments. Experimental studies on model systems for the splitting of thymine dimer radical cation have shown that the photodimer radical cation undergoes facile fragmentation reactions. Several experimental model studies have proposed a stepwise process.[12,14] Without depending on any suggestions from experimental data, we have obtained the reaction profile of the dimer splitting at the CASSCF level. The results of the present work support the stepwise mechanism: the dimer radical cation (TTp-1) undergoes the cleavage of the C6A−C6B bond to form the stretched bond isomer (TTp-2), followed by the cleavage of the C5A−C5B bond to form a thymine monomer and monomer radical cation (Figure 4). The energy barriers along the dissociation are low (see Table 2). The CASSCF level calculations have shown that the fragmentation reaction proceeds very easily once an electron is removed from thymine dimer. The calculated energy profile of the fragmentation reaction will change quantitatively with the level of the calculation employed. Other significant factors that will alter the current findings are the molecular environment in which the "real" fragmentation takes place, *i.e.*, DNA and solvent environments. It is likely, however, that the puckering of the four-membered ring in thymine dimer plays an essential element of the description of the fragmentation path, as observed here on the basis of the present CASSCF calculations.

Conclusion

The present study has addressed the fragmentation reaction of thymine dimer radical cation. It is demonstrated at the level of CASSCF calculations that the reaction is stepwise and proceeds easily with low-energy barriers. We have found that the puckering of the four-membered ring in thymine dimer determines the direction of the electron movement along the fragmentation.

Acknowledgment. The numerical calculations were carried out on the IBM/RS6000 Powerstations at the National Cancer Center Research Institute and on the SP2 at the computer center of the Institute for Molecular Science. This work was supported in part by a Grant-in Aid for Scientific Research from the Ministry of Education, Science and Culture.

Supporting Information Available: Tables for the cartesian coordinates of the stationary points along the fragmentation path of thymine dimer radical cation and their energies in hartrees (5 pages). See any current masthead page for ordering and Internet access instructions.

JA970184Q